

Electron dynamics controlled via self-interaction

Matteo Tamburini,^{1,*} Christoph H. Keitel,¹ and Antonino Di Piazza¹

¹*Max-Planck-Institut für Kernphysik, Saupfercheckweg 1, D-69117 Heidelberg, Germany*

(Dated: April 4, 2024)

The dynamics of an electron in a strong laser field can be significantly altered by radiation reaction. This usually results in a strongly damped motion, with the electron losing a large fraction of its initial energy. Here we show that the electron dynamics in a bichromatic laser pulse can be indirectly controlled by a comparatively small radiation reaction force through its interplay with the Lorentz force. By changing the relative phase between the two frequency components of the bichromatic laser field, an ultrarelativistic electron bunch colliding head-on with the laser pulse can be deflected in a controlled way, with the deflection angle being independent of the initial electron energy. The effect is predicted to be observable with laser powers and intensities close to those of current state-of-the-art petawatt laser systems.

PACS numbers: 41.20.-q, 41.60.-m, 41.75.Ht, 41.75.Jv

I. INTRODUCTION

The rapid progress of high-power laser systems has paved the way for the investigation of unexplored regimes of laser-matter interaction with a number of applications, e.g., in extreme field physics [1, 2], nuclear physics [3], hadron-therapy [4, 5] and relativistic laboratory astrophysics [6]. Next-generation 10-PW optical laser systems are expected to achieve intensities beyond 10^{23}W/cm^2 [2, 7], and laser pulses with power beyond 100 PW and intensity up to 10^{25}W/cm^2 are envisaged at the Extreme Light Infrastructure (ELI) [8] and at the eXawatt Center for Extreme Light Studies (XCELS) [9]. At such ultrahigh intensities, an electron becomes relativistic in a fraction of the laser period and its dynamics is dominated by radiation reaction (RR) effects, i.e., by the back reaction on the electron's motion of the radiation emitted by the electron itself while being accelerated by the laser pulse [10]. Hence, a deep understanding of RR effects is crucial for the design and the interpretation of future laser-matter experiments in the ultrarelativistic regime. Indeed, RR effects have several important implications ranging from the generation of high-energy photon [11–13], electron [14–16] and ion [17–21] beams, to the determination of bounds on particle acceleration in relativistic astrophysics [22, 23].

At available and upcoming laser intensities, RR effects become large for ultrarelativistic electrons, where the RR force basically amounts to a strongly nonlinear and anisotropic friction-like force [19]. This explains why all the proposals to experimentally test the underlying equation of motion [the so called Landau-Lifshitz (LL) [10] equation] rely on the RR-driven damping of the electron motion when an ultrarelativistic electron beam collides head-on with an intense laser pulse [11, 24–27]. However, the research to date has focused on revealing RR effects and understanding their fundamental features

rather than exploiting them in a possibly beneficial and controlled way.

In this paper, we show that RR effects can provide a route to the control of the electron dynamics via the non-linear interplay between the Lorentz and the RR force. This is achieved in a setup where an ultrarelativistic electron is exposed to a strong either few-cycle [28] or bichromatic [29] laser pulse. Our exact analytical calculations for a plane-wave pulse and our more realistic numerical simulations for a focused laser pulse show that, already at the intensities achievable with state-of-the-art laser systems, an ultrarelativistic electron colliding head-on with a bichromatic laser pulse can be deflected in an ultrafast and controlled way within a cone of about 8° aperture *independently* of the initial electron energy as long as quantum effects remain small. At still higher intensities, the interplay between the RR and the Lorentz force can even overcome the radiation losses themselves, resulting in a RR assisted electron acceleration instead of damping.

II. ELECTRON DYNAMICS IN AN ARBITRARY PLANE-WAVE FIELD

The LL equation of an electron (mass m and charge e) in the presence of an external electromagnetic field $F^{\mu\nu}$, is [10]:

$$\frac{du^\mu}{d\tau} = -F^{\mu\nu}u_\nu + r_R [F^{\mu\nu}F_{\nu\alpha}u^\alpha - (F^{\beta\nu}u_\beta F_{\nu\alpha}u^\alpha)u^\mu], \quad (1)$$

where τ is the proper time, $u^\mu \equiv dx^\mu/d\tau$ and where $r_R = 4\pi e^2/3mc^2\lambda \approx 1.18 \times 10^{-8}/\lambda_{\mu\text{m}}$, with λ being a typical length scale, conveniently chosen as the wavelength of a Ti:sapphire laser, i.e., $\lambda = 0.8 \mu\text{m}$. In Eq. (1) dimensionless units have been employed, such that time is in units of $\omega^{-1} \equiv \lambda/2\pi c$, length is in units of $\omega^{-1}c$, and fields are in units of $E^* \equiv m\omega c/|e|$. Note that the term of the RR force containing the derivatives of the field tensor $F^{\mu\nu}$ [10] has been neglected in Eq. (1) since its contribution is smaller than quantum effects [19] and

* matteo.tamburini@mpi-hd.mpg.de

it does not appreciably influence the electron dynamics in the regime of interest here.

Modeling the laser pulse as a plane wave propagating along the direction \vec{n} , the LL equation can be solved exactly for any plane-wave electromagnetic field which is an *arbitrary* function of the phase of the wave $\varphi = n_\mu x^\mu$ only, where $n^\mu \equiv (1, \vec{n})$ and $n^\mu n_\mu = 0$ [30]. Hereafter, the subscripts 0 and f refer to the initial and final value of the corresponding quantity, respectively. In order to analyze the origin of each term in the solution, we first omit the last term on the right-hand side of Eq. (1) (Larmor term). In this case $d\tau/d\varphi = 1/\rho_0$, where $\rho_0 \equiv n_\mu u_0^\mu$ is the initial Doppler factor and u_0^μ is the initial four-velocity. Inclusion of the Larmor term renders the relation between the proper time and the phase nonlinear [30]: $d\tau/d\varphi = h(\varphi)/\rho_0$ where $h(\varphi) = 1 + r_R \rho_0 \int_{\varphi_0}^{\varphi} [\vec{E}(\phi) \times \vec{B}(\phi)] \cdot \vec{n} d\phi$, with $\vec{E}(\phi)$ and $\vec{B}(\phi)$ being the plane wave electric and magnetic field, respectively. For an arbitrary plane wave, Eq. (1) written as a function of the phase φ becomes:

$$\frac{d\tilde{u}^\mu}{d\varphi} = -\frac{h}{\rho_0} F^{\mu\nu} \tilde{u}_\nu + \frac{h}{\rho_0^2} \frac{dh}{d\varphi} n^\mu, \quad (2)$$

where $\tilde{u}^\mu \equiv dx^\mu/d\varphi$. In Eq. (2), the only effect of the Larmor term is to multiply the terms in the right-hand side by $h(\varphi)$. Since $n_\mu F^{\mu\nu} = 0$, the solution of Eq. (2) is the sum of the two solutions obtained considering each term on the right-hand side of Eq. (2) separately. The second term in Eq. (2) results in a contribution proportional to $(h^2 - 1)n^\mu$. This term accounts for the effect of the radiation pressure [10] and leads to a small energy gain when an electron at rest is swept by a laser pulse [31, 32]. Finally, the first term on the right-hand side of Eq. (2) is a strongly nonlinear effective Lorentz force. This term can be integrated analytically, and the exact solution of Eq. (2) for the dimensionless four-momentum $p^\mu = (\varepsilon, \vec{p})$ as a function of φ is [30]:

$$\varepsilon = \frac{\varepsilon_0}{h} + \frac{2\vec{\mathcal{I}} \cdot \vec{p}_0 + (h^2 - 1) + \vec{\mathcal{I}}^2}{2\rho_0 h}, \quad (3)$$

$$\vec{p} = \frac{\vec{p}_0 + \vec{\mathcal{I}}}{h} + \frac{2\vec{\mathcal{I}} \cdot \vec{p}_0 + (h^2 - 1) + \vec{\mathcal{I}}^2}{2\rho_0 h} \vec{n}, \quad (4)$$

where $\vec{\mathcal{I}}(\varphi) = -\int_{\varphi_0}^{\varphi} h(\phi) \vec{E}(\phi) d\phi$. Since $\vec{E} \cdot \vec{n} = 0$, in Eq. (4) the vectors directed along \vec{n} and $\vec{\mathcal{I}}$ correspond to the longitudinal and transverse momentum gain, respectively.

Let us consider a bichromatic plane-wave pulse propagating along the positive z -axis and polarized along the x -axis with $E_x(\varphi) = g(\varphi) [\xi_1 \sin(\varphi + \theta_1) + \xi_2 \sin(2\varphi + \theta_2)]$, where $g(\varphi)$ is a smooth temporal envelope identically vanishing for φ outside the interval (φ_0, φ_f) , ξ_1, ξ_2 are the field amplitudes of each frequency component, and θ_1, θ_2 are two constant initial phases. After the electron passes through the laser beam, the relevant functions in the electron four-momentum are: $h_f = 1 + r_R \rho_0 \Psi$, $\mathcal{I}_{y,f} = 0$ and $\mathcal{I}_{x,f} = -r_R \rho_0 \Delta$, where $\Psi \equiv \int_{\varphi_0}^{\varphi_f} d\phi E_x^2(\phi)$,

$\Delta \equiv \int_{\varphi_0}^{\varphi_f} d\phi E_x(\phi) \int_{\varphi_0}^{\phi} d\vartheta E_x^2(\vartheta)$. For simplicity, in the following we assume a pulse envelope $g(\varphi) = \sin^2(\varphi/2N)$ in the interval $(0, \varphi_f)$ (i.e. $\varphi_0 = 0$), where $N = \varphi_f/2\pi$ is the total integer number of cycles of the pulse.

For the sake of comparison, we first consider a quasi-monochromatic plane wave ($\xi_2 = 0$ and $N \gg 1$). In this case, two frequencies are basically present in $E_x^2(\varphi)$, which arise from $\sin^2(\varphi + \theta_1)$. After integrating $E_x^2(\varphi)$, only the zero-frequency component provides a net contribution to Ψ . Analogously, the integrand of Δ only contains frequencies which are odd multiples of the central frequency ω , and Δ averages out to zero for a quasi-monochromatic plane wave. In fact, in our case

$$\Delta = \frac{3\pi\xi_1^3 N \cos(\theta_1)}{16(N^2 - 1)} \quad (N \geq 4), \quad (5)$$

which tends to zero for $N \rightarrow \infty$. The situation is essentially different for the bichromatic plane wave considered above. Here, a zero-frequency term arises in the integrand of Δ , such that Δ *diverges* in the limit $N \gg 1$:

$$\Delta \approx \frac{15\pi}{64} \xi_1^2 \xi_2 N \cos(\theta_2 - 2\theta_1) \quad (N \gg 1). \quad (6)$$

Recalling that $\mathcal{I}_{x,f} = -r_R \rho_0 \Delta$, Eqs. (4) and (6) already show *in general* that the electron dynamics can be controlled either by changing the constant initial phase $(\theta_2 - 2\theta_1)$ or the field amplitudes ξ_1, ξ_2 , and the effect dramatically increases for increasing ξ_1, ξ_2, N . Indeed, for $N \gg 1$ a different pulse envelope $g(\varphi)$ only alters the numerical factor on the right side of Eq. (6). Finally, we mention that $\mathcal{I}_{x,f}$ can become large also for ultraintense nearly one-cycle laser pulses [28]. However, in this case $\mathcal{I}_{x,f}$ is sensitive both to the carrier envelope phase θ_1 and to the precise shape of the pulse $g(\varphi)$.

Physically, without RR the electron transverse momentum $\vec{p}_\perp(\varphi) = \vec{p}(\varphi) - [\vec{n} \cdot \vec{p}(\varphi)]\vec{n}$ oscillates with the same frequencies as the plane-wave field [see Eq. (4) with $h(\varphi) = 1$]. Hence, the cumulative effect of the force eventually averages out to zero. However, the energy loss associated with the RR force modulates the position of the electron within the plane-wave field. For a quasi-monochromatic plane wave, there is no control on this modulation and thus no net transverse momentum gain [24, 27], as the modulation is intrinsically related to the frequency of the driving field. On the contrary, if a higher-frequency field is also included, its frequency and absolute phase can be chosen in such a way that a Fourier component is nonlinearly generated in the resulting modulation, which resonantly oscillates with the lower-frequency field. In turn, this resonance can result in a net transverse momentum gain $\delta p_x = \mathcal{I}_{x,f}/h_f$, and the interplay of the two components of the bichromatic field is indeed reflected in Eq. (6).

III. ELECTRON DYNAMICS CONTROL

Let us consider the effects arising from the interaction of an ultrarelativistic electron colliding head-on with a second-harmonic enriched laser pulse. Hereafter, the term $(h^2 - 1)$ in the numerator of Eqs. (3) and (4) is neglected in the analytical results, since it does not appreciably affect our conclusions. Eq. (4) indicates that the initially counterpropagating electron is deflected in the xz -plane asymmetrically. Since $\rho_0 \approx 2|\vec{p}_0|$, the deflection angle with respect to the initial propagation direction is

$$\zeta \approx -\arctan\left(\frac{2r_R\Delta}{1 - r_R^2\Delta^2}\right) \quad (7)$$

if $r_R|\Delta| < 1$, $\zeta + \pi$ if $r_R\Delta < -1$ and $\zeta - \pi$ if $r_R\Delta > 1$ *independently* of the initial electron energy. Again in the ultrarelativistic regime, for $r_R|\Delta| > 1$ the electron is back reflected by the plane-wave pulse. We stress that this condition is independent of the initial electron energy because higher initial energies imply higher RR effects, the functions h_f and $\vec{\mathcal{I}}_f$ being proportional to the initial Doppler factor ρ_0 . In other words, for $r_R|\Delta| > 1$ the laser pulse behaves like a perfectly reflecting electron “mirror”, i.e., it reflects back all the electrons with arbitrarily high initial energy, as long as the onset of quantum effects does not severely alter the predictions of classical electrodynamics (see below). In addition, from Eq. (3) it follows that if the initial electron energy ε_0 is less than $r_R\Delta^2/2\Psi$ then a surprising circumstance occurs: the final electron energy is *larger* than its initial energy. In fact, although the direct effect of the RR force is to reduce the electron energy, it also alters the temporal electron evolution, such that the electron’s world line with RR effects differs from the electron’s world line without them. As a result, while without RR effects the Lorentz force cannot perform a net work on the electron [see Eq. (3) with $h(\varphi) = 1$], with RR effects the Lorentz force can perform a positive work along the *RR-altered* electron world line. Hence, the dissipative RR force indirectly allows the Lorentz force to accelerate the electron, and when $\varepsilon_0 < r_R\Delta^2/2\Psi$ the indirect energy gain is larger than the direct energy loss. In order to observe this effect, an intensity beyond 10^{23} W/cm² and a waist radius of the order of some tens of micrometers are required, resulting in a power of the order of a few exawatts. Although such powers are well beyond those currently available, they may be achieved employing coherent beam superposition techniques [9, 33, 34].

IV. NUMERICAL RESULTS FOR A FOCUSED LASER PULSE

The above analytical predictions are exact if the laser field is modeled as a plane wave. In order to test them in a more realistic set-up, we solve Eq. (1) numerically for a focused laser pulse interacting with an electron bunch.

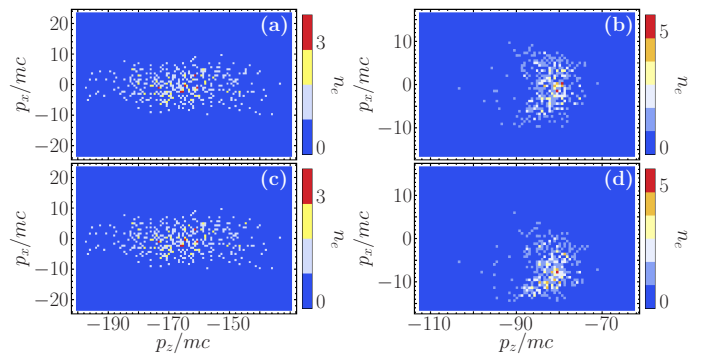


FIG. 1. (Color online) Electron density distribution $n_e(p_z, p_x)$ as a function of the longitudinal p_z and transverse p_x momentum after the interaction of 400 electrons with a bichromatic laser pulse. Panel (a): $\cos(\theta_2) = 0$ without RR. Panel (b): $\cos(\theta_2) = 0$ with RR. Panel (c): $\cos(\theta_2) = 1$ without RR. Panel (d): $\cos(\theta_2) = 1$ with RR. See the text for further numerical details.

Our simulations show that the plane-wave and the focused pulse results are in good agreement already with a $5\mu\text{m}$ waist radius (see below). Following Refs. [35, 36], a hyperbolic secant temporal envelope and a Gaussian transverse profile with terms up to the fifth order in the diffraction angle are employed to accurately describe the laser pulse, which reaches its maximal focusing at the origin with waist radius w_O . According to the notation employed so far, the laser beam stems from two pulses with wavelengths $0.8\mu\text{m}$ and $0.4\mu\text{m}$, respectively, and with peak field amplitudes ξ_1 and ξ_2 , respectively. Hereafter, for simplicity we set the constant phase $\theta_1 = 0$. The electrons are initially distributed according to a six-dimensional Gaussian probability distribution

$$f(\vec{x}, \vec{p}) = N_e \frac{e^{-\left[\frac{x^2+y^2}{2\sigma_T^2} + \frac{(z-z_0)^2}{2\sigma_L^2}\right] - \left[\frac{p_x^2+p_y^2}{2\sigma_{p_T}^2} + \frac{(p_z-p_{z,0})^2}{2\sigma_{p_L}^2}\right]}}{(2\pi)^3\sigma_T^2\sigma_{p_T}^2\sigma_L\sigma_{p_L}}, \quad (8)$$

with N_e being the total number of electrons and σ_T and σ_L (σ_{p_T} and σ_{p_L}) being the transverse and the longitudinal position (momentum) widths, respectively.

A. Simulation setup

In our simulation, the laser pulse is 70 fs long between its first and last half maximal intensity with $\xi_1 = 40$ (3.4×10^{21} W/cm²), $\xi_2 = 28$ (1.7×10^{21} W/cm²) and the waist radius is $w_O = 5\mu\text{m}$. Hence, the total intensity and power are 5.1×10^{21} W/cm² and 2 PW, respectively. Initially, the electron bunch has mean momentum $p_{z,0} = -165 mc$ with standard deviations $\sigma_T = 0.2\mu\text{m}$, $\sigma_L = 0.5\mu\text{m}$, $\sigma_{p_T} = 1 mc$ and $\sigma_{p_L} = 12 mc$. The electron average density is $3 \times 10^{15}\text{cm}^{-3}$ so that the electron bunch contains about 400 electrons. The above-mentioned laser parameters are similar to those of available petawatt laser systems [2, 7]. Much larger effects

can be achieved at higher intensities, since the transverse momentum gain increases rapidly with rising laser field amplitudes ξ_1, ξ_2 [see Eq. (6)]. In addition, the electron deflection can be controlled by changing either the phase θ_2 or the amplitudes ξ_1, ξ_2 . The latter approach can be exploited tuning the ratio between ξ_1 and ξ_2 by controlling the second-harmonic conversion efficiency, e.g., by changing the tilt angle in a tilted-crystal configuration [37]. To date, frequency-doubling efficiencies up to 73% at 2 TW/cm² intensity have been demonstrated experimentally for femtosecond pulses [29]. Also, phase-control of bichromatic laser pulses has been employed at intensities of the order of 10¹⁴ W/cm² to steer the electron dynamics in nonrelativistic atomic physics [38]. Similar techniques might be extended to higher intensities via coherent beam superposition of multiple laser beams [9, 33, 34], since a relatively compact optics can be employed for each amplification channel. Finally, electron bunches with the same parameters as in our simulation have been generated experimentally employing standard multiterawatt optical lasers [39]. Such relatively low-power pulses can also be generated by extracting a fraction of energy from the initial strong pulse before the frequency-doubling.

B. Results and discussion

Figure 1 reports the electron density distribution $n_e(p_z, p_x)$ as a function of the longitudinal p_z and transverse p_x momentum for the interaction of 400 electrons with the focused laser pulse both for $\cos(\theta_2) = 0$ and $\cos(\theta_2) = 1$, with and without RR. No appreciable difference between $\cos(\theta_2) = 0$ and $\cos(\theta_2) = 1$ is found if only the Lorentz force is taken into account. Furthermore, if the RR force is neglected, the mean of the momentum distribution remains unaltered after the electron bunch has passed through the laser pulse $\bar{p}_x \approx 0$ and $\bar{p}_z \approx -165 mc$ [see Figs. 1(a), 1(c)]. However, if the RR force is taken into account, for $\cos(\theta_2) = 0$ the electrons still move along their initial propagation direction and are distributed symmetrically in the transverse momentum space with $\bar{p}_x \approx 0$ and $\bar{p}_z \approx -82 mc$ [see Fig. 1(b)] in good agreement with the plane wave prediction $p_{x,f} \approx 0$ and $p_{z,f} \approx -79 mc$. On the other hand, for $\cos(\theta_2) = 1$ all the electrons are deflected in the transverse direction independently of their initial energy, the mean of the momentum distributions being $\bar{p}_x \approx -7 mc$ and $\bar{p}_z \approx -82 mc$ [see Fig. 1(d)]. For the corresponding plane-wave pulse, we obtain $p_{x,f} \approx -5.8 mc$ and $p_{z,f} \approx -79 mc$, in good agreement with the above mentioned focused pulse results.

The effect of QED corrections to the classical prediction has been estimated by introducing a quantum corrected RR force, which accounts for the reduction of the emitted power in the quantum case compared to the classical one [40]. The present approach is valid as long as the quantum parameter $\chi = |e|\hbar\sqrt{[F^{\mu\nu}p_\nu]^2}/m^3c^4$ (Gaus-

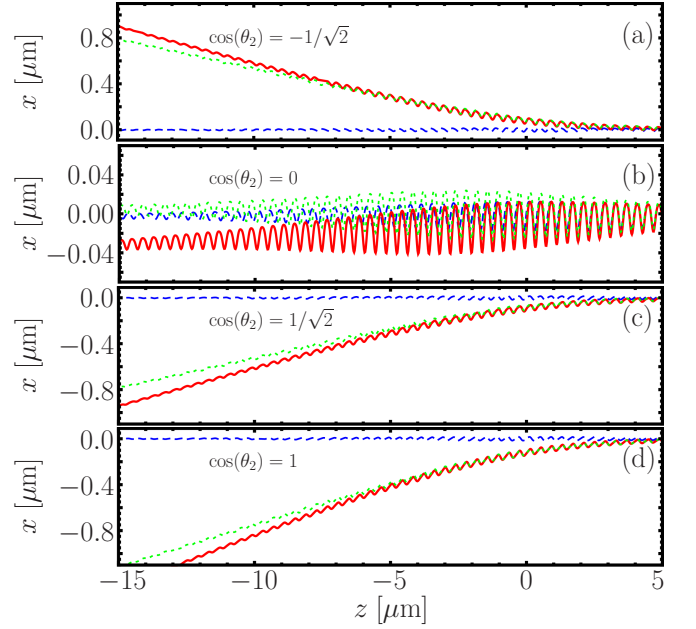


FIG. 2. (Color online) Trajectory of an electron colliding head-on with a bichromatic laser pulse without (blue dashed line) and with (red solid line) RR force included. The corresponding plane wave result with RR (green dotted line) is also reported for comparison. In all cases $\theta_1 = 0$. Panel (a): $\cos(\theta_2) = -1/\sqrt{2}$. Panel (b): $\cos(\theta_2) = 0$. Panel (c): $\cos(\theta_2) = 1/\sqrt{2}$. Panel (d): $\cos(\theta_2) = 1$. See the text for further numerical details.

sian units) remains much smaller than unity [2, 40]. Indeed, in our simulations we found $\chi \lesssim 0.04$. Moreover, due to RR effects, χ remains significantly smaller compared to the case without RR, especially at higher laser pulse intensities. In our simulation, quantum corrections do not qualitatively affect the results but induce a correction to the final mean momenta of the electron distribution, with $\bar{p}_x \approx 0$ and $\bar{p}_z \approx -87 mc$ for $\cos(\theta_2) = 0$, and $\bar{p}_x \approx -6 mc$ and $\bar{p}_z \approx -88 mc$ for $\cos(\theta_2) = 1$. Finally, stochasticity effects in quantum RR may broaden the final electron distribution but do not significantly alter its mean value [41].

Figure 2 displays the trajectory of an electron injected into the focus of the bichromatic laser pulse with initial momentum $\vec{p}_0 = (0, 0, -165 mc)$ without (blue dashed line) and with (red solid line) RR effects included [the corresponding plane wave result with RR (green dotted line) is also shown for comparison]. In all cases, the electron passes through the laser pulse without changing its initial propagation direction when RR effects are neglected. When RR effects are included, for $\cos(\theta_2) = 0$ the electron goes through the laser pulse without significantly deviating from its initial propagation direction [see Fig. 2(b)], whereas it is quickly deflected in the transverse direction for $\cos(\theta_2) \neq 0$ [see Figs. 2(a), 2(c) and 2(d)]. From Eq. (7) with $\cos(\theta_2) = 1$ [$\cos(\theta_2) = \mp 1/\sqrt{2}$], the predicted deflection angle for the plane-wave becomes

$\zeta \approx -4.2^\circ$ ($\zeta \approx \pm 3^\circ$) in fair agreement with the focused pulse result $\zeta \approx -5.4^\circ$ ($\zeta \approx \pm 3.8^\circ$). Quantum effects lead to relatively small corrections, the deflection angle being $\zeta \approx -3.6^\circ$ ($\zeta \approx \pm 2.5^\circ$) for the plane wave with $\cos(\theta_2) = 1$ [$\cos(\theta_2) = \mp 1/\sqrt{2}$] and $\zeta \approx -4.5^\circ$ ($\zeta \approx \pm 3.2^\circ$) for the focused pulse.

ACKNOWLEDGMENTS

We acknowledge useful discussions with N. Neitz, G. Sarri, and A. M. Sergeev.

-
- [1] F. Ehlotzky, K. Krajewska, and J. Z. Kamiński, Rep. Prog. Phys. **72**, 046401 (2009).
 - [2] A. Di Piazza, C. Müller, K. Z. Hatsagortsyan, and C. H. Keitel, Rev. Mod. Phys. **84**, 1177 (2012).
 - [3] K. W. D. Ledingham, P. McKenna, and R. P. Singhal, Science **300**, 1107 (2003).
 - [4] S. D. Kraft, C. Richter, K. Zeil, M. Baumann, E. Beyreuther, S. Bock, M. Bussmann, T. E. Cowan, Y. Dammene, W. Enghardt, U. Helbig, L. Karsch, T. Kluge, L. Laschinsky, E. Lessmann, J. Metzkes, D. Naumburger, R. Sauerbrey, M. Schrer, M. Sobiella, J. Woithe, U. Schramm, and J. Pawelke, New J. Phys. **12**, 085003 (2010).
 - [5] Y. I. Salamin, Z. Harman, and C. H. Keitel, Phys. Rev. Lett. **100**, 155004 (2008).
 - [6] S. V. Bulanov, T. Z. Esirkepov, D. Habs, F. Pegoraro, and T. Tajima, Eur. Phys. J. D **55**, 483 (2009).
 - [7] A. V. Korzhimanov, A. A. Gonoskov, E. A. Khazanov, and A. M. Sergeev, Phys. Usp. **54**, 9 (2011).
 - [8] “Extreme light infrastructure,” <http://www.extreme-light-infrastructure.eu> (2013).
 - [9] “Exawatt center for extreme light studies,” <http://www.xcels.iapras.ru> (2013).
 - [10] L. D. Landau and E. M. Lifshitz, “The classical theory of fields,” (Pergamon Press, Oxford, 1971) Chap. 76, 78, 3rd ed.
 - [11] J. Koga, T. Z. Esirkepov, and S. V. Bulanov, Phys. Plasmas **12**, 093106 (2005).
 - [12] T. Nakamura, J. K. Koga, T. Z. Esirkepov, M. Kando, G. Korn, and S. V. Bulanov, Phys. Rev. Lett. **108**, 195001 (2012).
 - [13] C. P. Ridgers, C. S. Brady, R. Duclous, J. G. Kirk, K. Bennett, T. D. Arber, A. P. L. Robinson, and A. R. Bell, Phys. Rev. Lett. **108**, 165006 (2012).
 - [14] P. Michel, C. B. Schroeder, B. A. Shadwick, E. Esarey, and W. P. Leemans, Phys. Rev. E **74**, 026501 (2006).
 - [15] I. Y. Kostyukov, E. N. Nerush, and A. G. Litvak, Phys. Rev. ST Accel. Beams **15**, 111001 (2012).
 - [16] C. H. Keitel, C. Szymanowski, P. L. Knight, and A. Maquet, J. Phys. B **31**, L75 (1998).
 - [17] N. Naumova, T. Schlegel, V. T. Tikhonchuk, C. Labaune, I. V. Sokolov, and G. Mourou, Phys. Rev. Lett. **102**, 025002 (2009).
 - [18] T. Schlegel, N. Naumova, V. T. Tikhonchuk, C. Labaune, I. V. Sokolov, and G. Mourou, Phys. Plasmas **16**, 083103 (2009).
 - [19] M. Tamburini, F. Pegoraro, A. Di Piazza, C. H. Keitel, and A. Macchi, New J. Phys. **12**, 123005 (2010).
 - [20] M. Chen, A. Pukhov, T.-P. Yu, and Z.-M. Sheng, Plasma Phys. Control. Fusion **53**, 014004 (2011).
 - [21] M. Tamburini, T. V. Liseykina, F. Pegoraro, and A. Macchi, Phys. Rev. E **85**, 016407 (2012).
 - [22] F. A. Aharonian, A. A. Belyanin, E. V. Derishev, V. V. Kocharovskiy, and V. V. Kocharovskiy, Phys. Rev. D **66**, 023005 (2002).
 - [23] M. V. Medvedev, Phys. Rev. E **67**, 045401 (2003).
 - [24] A. Di Piazza, K. Z. Hatsagortsyan, and C. H. Keitel, Phys. Rev. Lett. **102**, 254802 (2009).
 - [25] C. Harvey, T. Heinzl, and M. Marklund, Phys. Rev. D **84**, 116005 (2011).
 - [26] C. Harvey and M. Marklund, Phys. Rev. A **85**, 013412 (2012).
 - [27] A. G. R. Thomas, C. P. Ridgers, S. S. Bulanov, B. J. Griffin, and S. P. D. Mangles, Phys. Rev. X **2**, 041004 (2012).
 - [28] M. Tamburini, A. Di Piazza, T. V. Liseykina, and C. H. Keitel, ArXiv e-prints (2012), arXiv:1208.0794.
 - [29] S. Y. Mironov, V. N. Ginzburg, V. V. Lozhkarev, G. A. Luchinin, A. V. Kirsanov, I. V. Yakovlev, E. A. Khazanov, and A. A. Shaykin, Quantum Electron. **41**, 963 (2011).
 - [30] A. Di Piazza, Lett. Math. Phys. **83**, 305 (2008).
 - [31] D. M. Fradkin, Phys. Rev. Lett. **42**, 1209 (1979).
 - [32] G. Lehmann and K. H. Spatschek, Phys. Rev. E **84**, 046409 (2011).
 - [33] S. N. Bagayev, V. I. Trunov, E. V. Pestryakov, S. A. Frolov, V. E. Leschenko, A. V. Kirpichnikov, A. E. Kokh, V. V. Petrov, and V. A. Vasiliev, AIP Conf. Proc. **1465**, 18 (2012).
 - [34] G. Mourou, B. Brocklesby, T. Tajima, and J. Limpert, Nature Photon. **7**, 258 (2013).
 - [35] K. T. McDonald, “<http://hep.princeton.edu/mcdonald/accel/gaussian2.pdf>,” (1997).
 - [36] Y. I. Salamin and C. H. Keitel, Phys. Rev. Lett. **88**, 095005 (2002).
 - [37] K. Mori, Y. Tamaki, M. Obara, and K. Midorikawa, J. Appl. Phys. **83**, 2915 (1998).
 - [38] S. Watanabe, K. Kondo, Y. Nabekawa, A. Sagisaka, and Y. Kobayashi, Phys. Rev. Lett. **73**, 2692 (1994); J. Mauritsson, P. Johnsson, E. Gustafsson, A. L’Huillier, K. J. Schafer, and M. B. Gaarde, Phys. Rev. Lett. **97**, 013001 (2006); H. Xu, W. Chu, Y. Liu, W. Liu, H. Xiong, Y. Fu, J. Yao, B. Zeng, J. Ni, S. Chin, Y. Cheng, and Z. Xu, Appl. Phys. B **104**, 909 (2011).
 - [39] O. Lundh, J. Lim, C. Rechatin, L. Ammouira, A. Ben-Ismaïl, X. Davoine, G. Gallot, J.-P. Goddet, E. Lefebvre, V. Malka, and J. Faure, Nature Phys. **7**, 219 (2011).
 - [40] V. N. Baier, V. M. Katkov, and V. M. Strakhovenko, *Electromagnetic Processes at High Energies in Oriented Single Crystals* (World Scientific, Singapore, 1998).
 - [41] N. Neitz and A. Di Piazza, Phys. Rev. Lett. **111**, 054802 (2013).